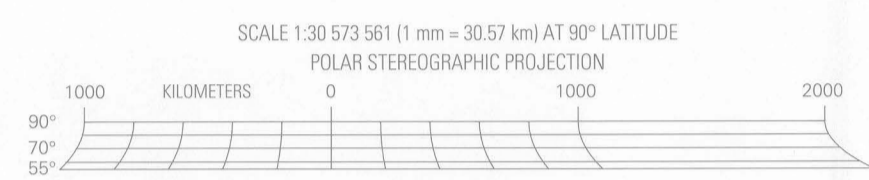


NORTH POLAR REGION



NOTES ON BASE
This sheet is one in a series of maps of Venus at nominal scales of 1:50,000,000 and 1:10,000,000 (Planetary Cartography Working Group, 1984 and 1993; Batson and others, 1994). It is based on data from the Magellan Synthetic Aperture Radar (SAR) instrument. The Magellan Mission was described by Saunders and Pettengill (1991). Magellan radar characteristics were described by Pettengill and others (1991).

ADOPTED FIGURE
The figure of Venus used for the computation of the map projection is a sphere with a mean radius of 6,051.0 km, consistent with the preliminary gravity figure reported by Phillips and others (1979) that was used for previous maps of Venus. Slightly larger values of the mean radius of Venus have subsequently been reported based on Pioneer Venus (Pettengill and others, 1980) and Magellan altimetry (Ford and Pettengill, 1992).

PROJECTION
The Mercator projection is used for the polar regions north and south of the 55° parallels. The scale is 1:50,000,000 at lat 0° (Mercator) and 1:30,573,561 at ±90° (polar stereographic); both projections share a common scale of 1:27,959,645 at lat ±55°. Due to the retrograde rotation of Venus, longitude increases from west to east in accordance with usage of the International Astronomical Union (1971).

CONTROL
Planimetric control is derived from the radio-tracked position of the spacecraft. The first meridian passes through the central peak of the eastern Atlatius, at lat 43.8° N, according to current International Astronomical Union convention. (Atlatius replaces the feature "Eve," which, at the same longitude, originally fixed the location of the prime meridian Davies and others, 1986.) The Venusian cartographic coordinate system was described by Davies and others (1992).

MAPPING TECHNIQUES
Magellan SAR datasets were originally produced by the Jet Propulsion Laboratory. Full-resolution (75 m/px) image strips were compressed and mosaicked to produce CI-MIDR's (Compressed-Over-Mosaicked Image Data Record, 225 m/px) (Pettengill and others, 1991). CI-MIDR's were assembled and reprojected to produce this map. Cycles 1 and 2 left (east)-looking, Cycle 2 and 3 right (west)-looking, and Cycle 3 left (east)-looking with reduced (stereo) incidence angle data records were used in the image mosaic. (Cycle 1 radar operations commenced September 15, 1990, and ended May 16, 1991; Cycle 2 began May 16, 1991, and ended January 17, 1992; Cycle 3 began January 17, 1992, and ended September 13, 1992.)
Cartographic processing was done by Robert M. Sucharski.

SYNTHETIC APERTURE RADAR (SAR) IMAGE INTERPRETATION
Because side-looking radar uses long-wave radiation and an imaging geometry distinct from that of framing camera radar images differ from conventional photographs (Ford and others, 1993, p. 45-56; and Young, 1990, p. 71). These differences should be kept in mind when interpreting radar images. Brightness in radar images is dependent on three factors: topography, surface texture, and surface electrical properties.
Topography affects radar images as it affects photographs. Surfaces sloping toward the source of illumination appear brighter and surfaces sloping away appear darker. However, note that the source of illumination for SAR radar images, the radar transmitter, is the same as the site of the observation, the receiving antenna (fig. 2). This geometry gives SAR images a different perspective from most photographs, where the illumination source (usually the sun) is independent of the observing position. Relief properties are most effectively seen in SAR images when they are relatively abrupt. Shallow slopes are not shown well on SAR images.
Surface texture strongly affects radar brightness yet may have little effect in photographic images. Surfaces whose roughness is comparable with the radar wavelength (12.6 cm for Magellan; Pettengill and others, 1991) scatter more energy back to the radar receiver (they appear brighter) than do smooth, mirror-like surfaces, or surfaces composed of very small particles such as sand or silt, which will be transparent to or, if of sufficient depth, absorb radar waves (appear dark). Thus, areas that appear dark in a photo-

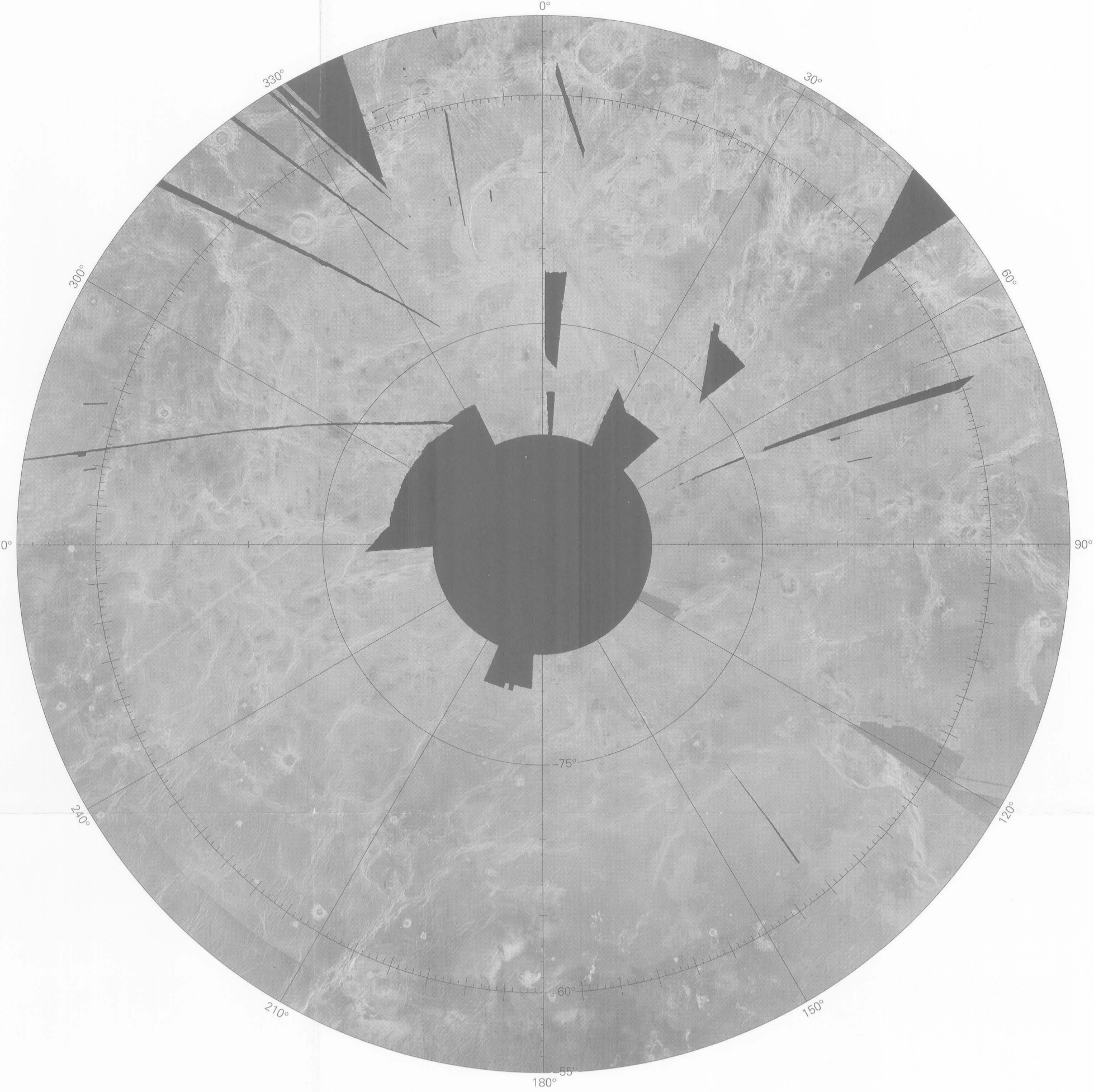
graph may be bright in a radar image, and vice versa.

The third major influence on radar brightness is due to the electrical properties of the surface: materials having higher dielectric constants reflect radio waves more strongly, and hence appear brighter, than materials having low dielectric constants. Variations in dielectric constants over most of Venus are subtle, and their influence on image brightness is generally overwhelmed by that of relief or roughness variations. However, brightness is significantly enhanced planet-wide for materials at elevations above a radius of about 6,055 km (Tyler and others, 1991). The electric properties are dependent on frequency; high reflectivity in the radar images does not necessarily correlate with high reflectivity in the optical part of the spectrum.

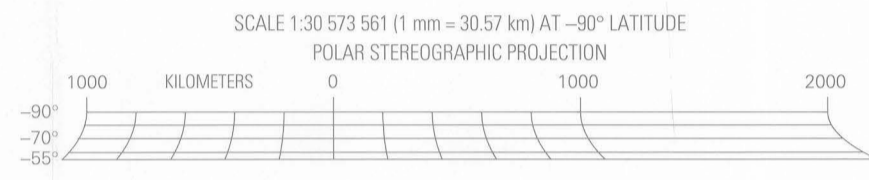
The side-looking geometry of imaging radar leads to geometric distortion ("bow-wow" of features with significant relief). Slopes facing the radar appear foreshortened. In extreme cases, where the slope angle exceeds the incidence angle (fig. 2) the radar echo from the base of the slope is received before the echo from the top so that the surface may even appear to be folded back upon itself. Correspondingly, slopes facing away from the radar appear elongated. The amount of bow-wow increases with decreasing incidence angle; the incidence angle used by Magellan as a function of latitude is shown in figure 3. Greatly expanded explanations of these effects, as well as summaries of Magellan operations and Venusian geology, can be found in the Magellan Venus Explorer's Guide (Young and others, 1990) and in the Guide to Magellan Image Interpretation (Ford and others, 1993). The latter is substantially more technical.

NOMENCLATURE
V 50M 0/0 CM. Abbreviation for Venus, 1:50,000,000 series; center of map, lat 0°, long 0°; controlled mosaic (CM).

REFERENCES CITED
Batson, R.M., Kirk, R.L., Edwards, K.F., and Morgan, H.F., 1994, Venus cartography: Journal of Geophysical Research, v. 99, p. 21,173-21,182.
Davies, M.E., and nine others, 1986, Report of the IAU/AG/COSPAR Working Group on Cartographic Coordinates and Rotational Elements of the Planets and Satellites, Celestial Mechanics, no. 39, p. 103-113.
Davies, M.E., and eight others, 1992, The rotation period, direction of the north pole, and geodetic control network of Venus. Journal of Geophysical Research, v. 97, no. E8, p. 13,141-13,151.
Ford, J.P., and seven others, 1993, Guide to Magellan Image Interpretation. Jet Propulsion Laboratory publication 93-24, 148 p.
Ford, P.G., and Pettengill, G.H., 1992, Venus topography and kilometer-scale slopes: Journal of Geophysical Research, v. 97, p. 13,103-13,114.
International Astronomical Union, 1971, Commission 16: Physical study of planets and satellites, in Proceedings of the 14th General Assembly, Brighton, 1970. Transactions of the International Astronomical Union, v. 14B, p. 128-137.
Pettengill, G.H., and five others, 1980, Pioneer Venus radar results: Altimetry and surface properties. Journal of Geophysical Research, v. 85, no. A13, p. 82,261-82,270.
Pettengill, G.H., and four others, 1991, Magellan: Radar performance and data products. Science, v. 252, no. 5003, p. 240-245.
Phillips, R.J., and five others, 1979, The gravity field of Venus: A preliminary analysis. Science, v. 205, no. 4401, p. 93-96.
Planetary Cartography Working Group (Strom, R.G., and ten others), 1984, Planetary cartography in the next decade (1984-1994). National Aeronautics and Space Administration Special Publication 475, 71 p.
Planetary Cartography Working Group (Zimbleman, J.R., and sixteen others), 1993, Planetary cartography 1993-2003. National Aeronautics and Space Administration, Planetary Cartography Working Group, 50 p.
Saunders, R.S., and Pettengill, G.H., 1991, Magellan: Mission summary. Science, v. 252, no. 5003, p. 247-249.
Tyler, G.L., Ford, P.G., Campbell, D.B., Elachi, C., Pettengill, G.H., and Simpson, R.A., 1991, Magellan: Electrical and physical properties of Venus' surface. Science, v. 252, p. 265-270.
Young, Carolyn, ed., 1990, The Magellan Venus Explorer's Guide: Jet Propulsion Laboratory publication 90-24, 197 p.



SOUTH POLAR REGION



SCALE 1:50,000,000 (1 mm = 50 km) AT 0° LATITUDE
MERCATOR PROJECTION

INTERIOR - GEOLOGICAL SURVEY, RESTON, VA - 20192
Prepared on behalf of the NASA Planetary Geology and Geophysics program and the Magellan Project Office of the Jet Propulsion Laboratory. Edited by Dietrich Hiesh; cartography by Roger D. Canoll. Manuscript approved for publication August 18, 1993.

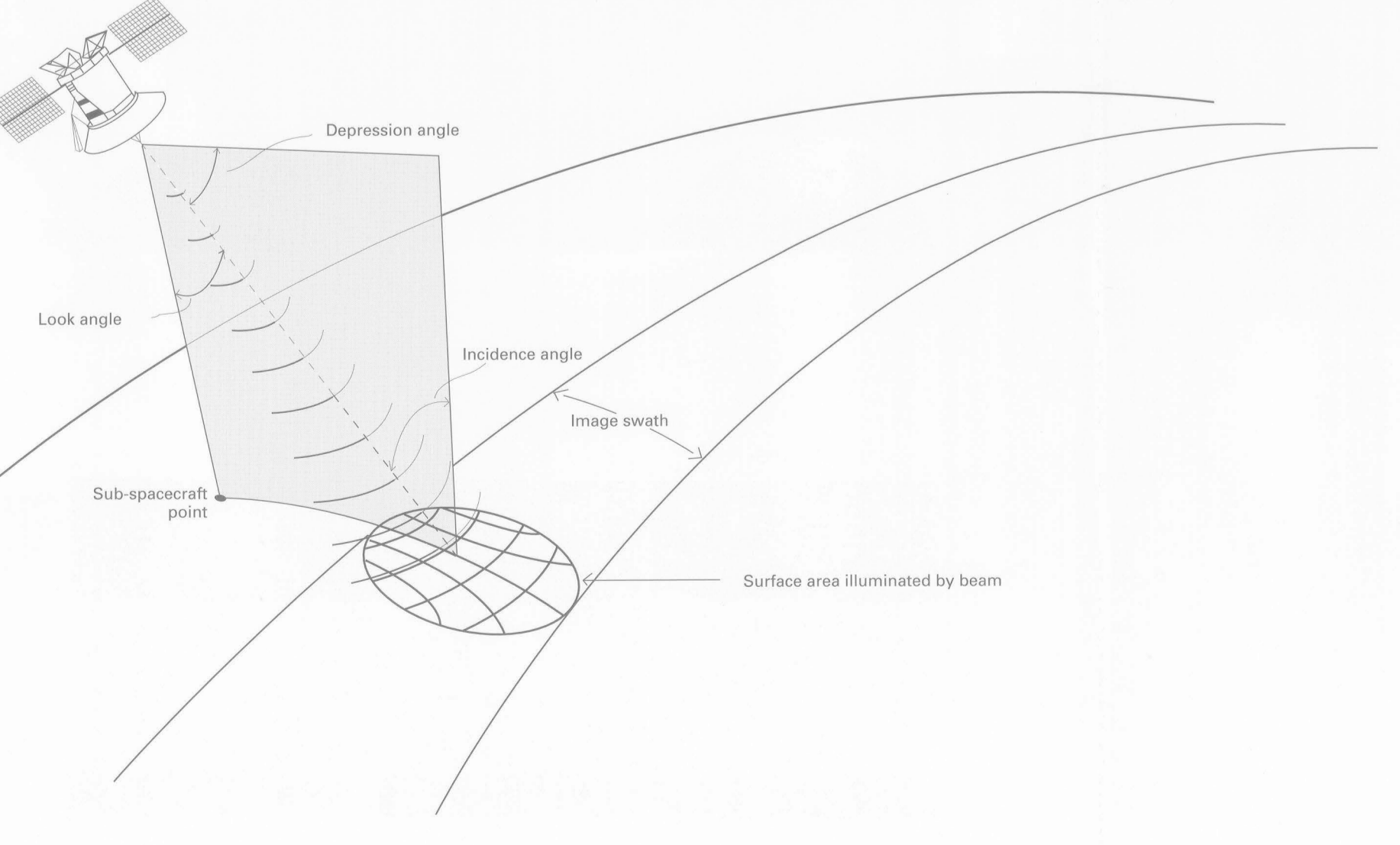
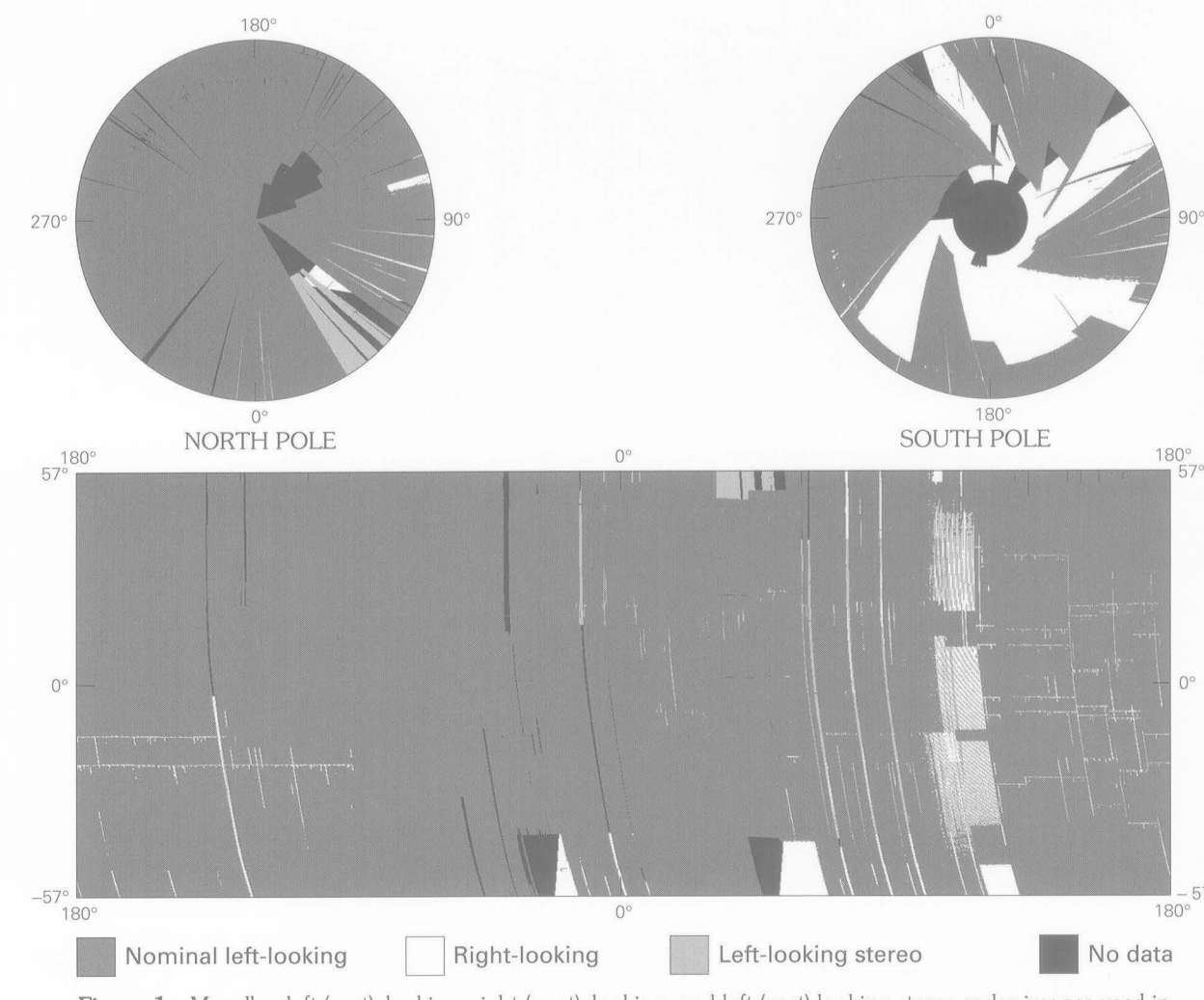


Figure 2. Geometry of the Magellan Synthetic Aperture Radar (SAR) footprint and terminology.

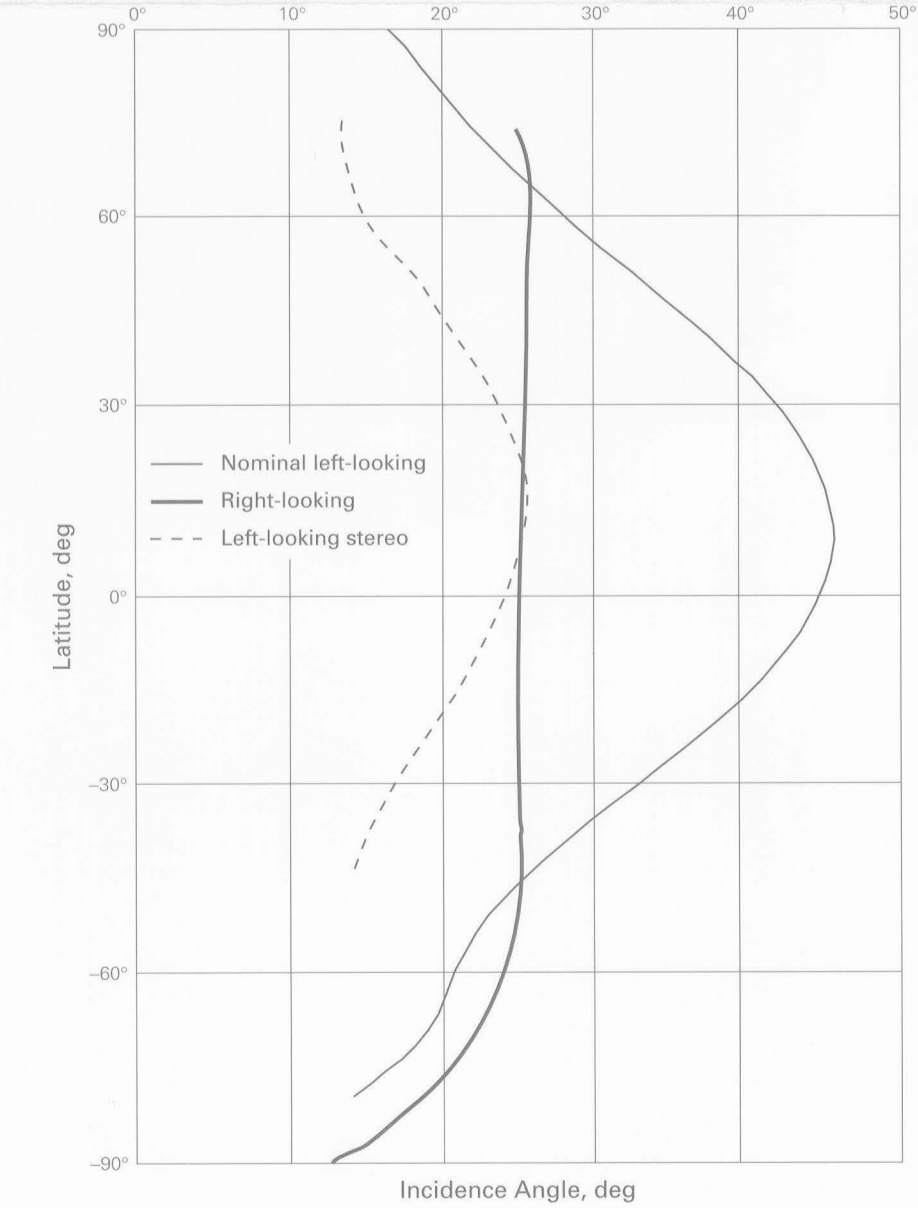
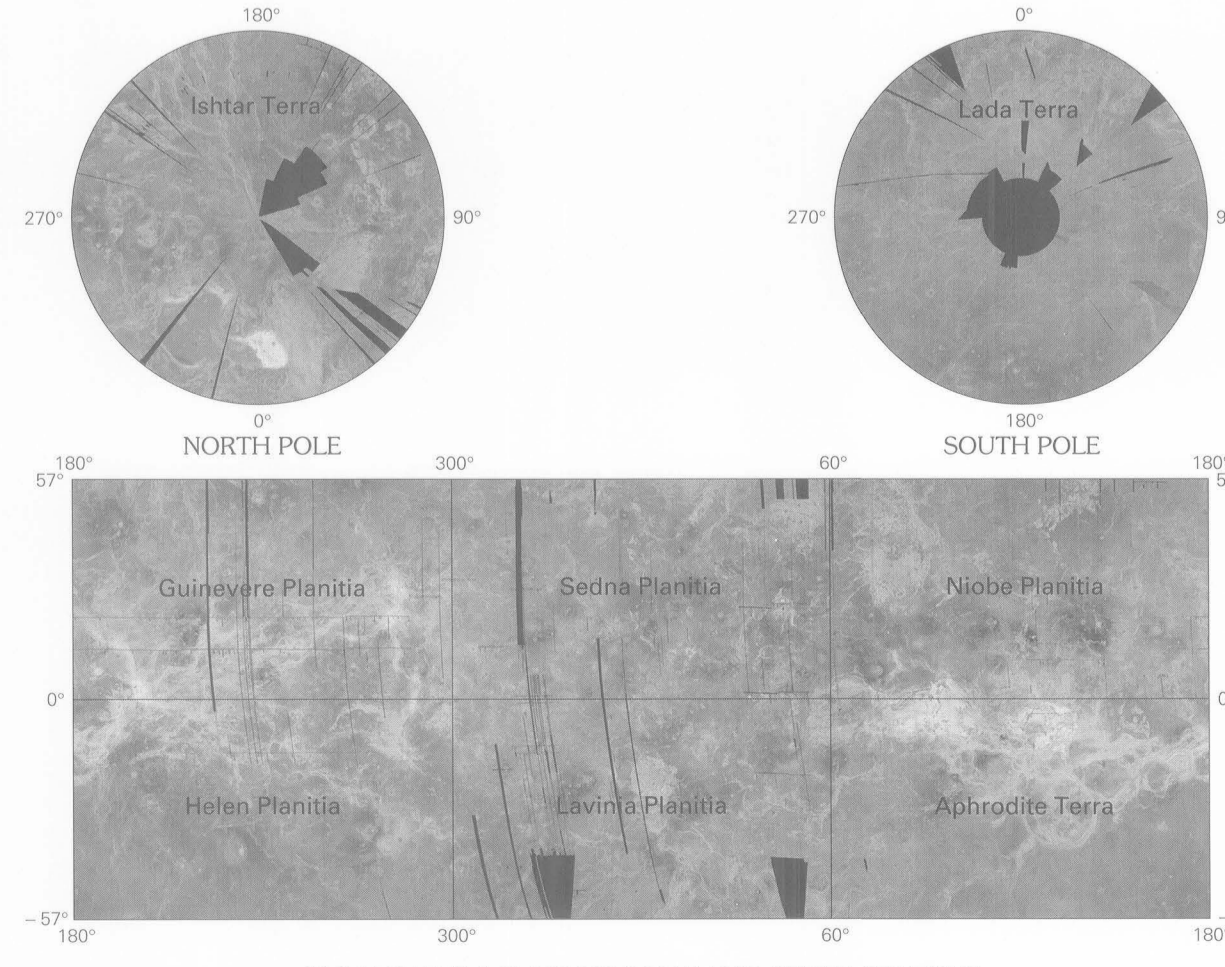


Figure 3. Magellan radar incidence angles as a function of latitude. Spacecraft look angle was varied during right-looking operations to keep the nominal incidence angle at about 25°. Nominal incidence angle was reduced during part of left-looking operations to produce optimal stereo viewing geometry in combination with normal left-looking images.



INDEX OF THE 1:10,000,000 SCALE MAP SERIES OF VENUS

RADAR IMAGE MAP OF VENUS

V 50M 0/0 CM
1997

ISBN 0-607-88747-8
9 780607 887471
For sale by U.S. Geological Survey, Information Services, Box 25288, Federal Center, Denver, CO 80225

NOTE TO USERS
Users noting errors or omissions are urged to indicate them on the map and to forward it to U.S. Geological Survey, Building 4, Room 450, 2255 N. Gemini Drive, Flagstaff, AZ 86001. A replacement copy will be returned.